Robust control of unstable nonlinear quantum systems

Jing-Jun Zhu [1,2] Xi Chen [1,2,3,*] Hans-Rudolf Jauslin [4] and Stéphane Guérin [4,†]

[1] *International Center of Quantum Artificial Intelligence for Science and Technology (QuArtist), Shanghai University, 200444 Shanghai, China*

[2] *Department of Physics, Shanghai University, 200444 Shanghai, China*

[3] *Department of Physical Chemistry, University of the Basque Country, 48080 Bilbao, Spain*

[4] *Laboratoire Interdisciplinaire Carnot de Bourgogne, CNRS UMR 6303, Université de Bourgogne Franche-Comté, BP 47870, 21078 Dijon, France*

(Received 26 May 2020; revised 3 October 2020; accepted 5 October 2020; published 4 November 2020)

Adiabatic passage is a standard tool for achieving robust transfer in quantum systems. We show that in driven nonlinear quantum systems adiabatic passage becomes highly *nonrobust* when the target is unstable. This occurs for a generic (1:2) resonance, for which the complete transfer corresponds to a hyperbolic fixed point featuring an adiabatic connectivity strongly sensitive to small perturbations of the model. By inverse engineering, we devise high-fidelity and robust partially nonadiabatic trajectories. They localize at the approach of the target near the stable manifold of the separatrix, which drives the dynamics towards the target in a robust way. These results can be applicable to atom-molecule Bose-Einstein condensate conversion and to nonlinear optics.

DOI: 10.1103/PhysRevA.102.052203

I. INTRODUCTION

Development of quantum control is an essential task for quantum technology [1,2]. Quantum control means manipulating dynamical processes of quantum systems, via the control of their states aiming typically the transfer from one to another state, using external fields. Besides requirements of high-fidelity transfer, an important issue is the robustness of the control, for instance, with respect to imperfect knowledge of the system or to systematic deviations in experimental parameters. Adiabatic passage is a well-known technique for achieving robust transfer [3]. Other robust techniques have been demonstrated, such as composite pulses [4,5], optimal control [6,7], or single-shot shaped pulses [8,9] as a variant of shortcut to adiabaticity [10–13].

Nonlinear quantum systems are central in recent applications, such as the ones involving many-particle systems in a mean field [14–16] or nonlinear optics [17–21], but little is known about the applicability of the control principles developed for linear systems. Since the corresponding Hamiltonian depends on the state of the system, nonlinear quantum dynamics can be described by Hamilton's equations with a nonlinear Hamiltonian, from which issues of instabilities and nonintegrability are expected to feature obstructions of control [22,23].

Adiabatic passage techniques can be formulated for integrable systems with trajectories formed by the instantaneous (stable) elliptic fixed points defined at each value of the adiabatic parameters and continuously connected to the initial condition. Obstructions to classical adiabatic passage are given by the crossing of a separatrix [22,24,25]. Besides optimal control based on Pontryagin's maximum principle [26–28], the use of inverse engineering techniques allows one to produce exact solutions without the need of invoking adiabatic approximations [29]. Two- and three-level Λ-type systems with second-order nonlinearities have been shown to be noncontrollable exactly in the sense that such nonlinearities prevent reaching the target state exactly [24,29]. However, one can approach it as closely as required, and inverse-engineering techniques have been developed for that purpose [29].

However, when the target state is itself unstable, e.g., associated to an hyperbolic fixed point in the classical phase space representation, as it is the case for a two-level system with a generic (1:2) resonance, we show the counterintuitive result that *adiabatic solutions lack robustness*.

We note that this results was not noticed in literature dedicated to adiabatic passage in nonlinear systems even if robustness was analyzed. We can mention Ref. [24] where a relative robustness was apparent but only in a restricted zone of parameters. In conventional nonlinear Λ three-level systems, where the (1:2) nonlinearity is only for the transition involving the initial state (traditionally associated to a pump coupling), one can derive robust solutions by imposing that the transient population in the upper state is small, in a similar way as for its linear counterpart [29]. Robustness can be naturally achieved in such systems because the target state, linked with a linear Stokes coupling, is stable in the phase space [22]. This is also the case for two-level systems featuring only third-order nonlinearity [28]. We can finally mention that nonintegrability can be circumvented by appropriate design of pulse's parameters [23].

The existence of robust solutions for a (1:2) resonance becomes then questionable. The goal of this paper is to analyze the obstruction of adiabatic passage and to design such robust trajectories, using inverse engineering adapted to nonlinear dynamics.

*xchen@shu.edu.cn

†sguerin@u-bourgogne.fr

 ©2020 American Physical Society

In Sec. II we present the model and the underlying Bloch sphere generalized to nonlinear systems, on which the solutions will be interpreted as trajectories. In Sec. III we show the nonrobustness of adiabatic passage. In Sec. IV we show robust solutions designed from reverse engineering methods. The last section is devoted to the conclusion.

II. NONLINEAR (1:2) RESONANCE MODEL AND THE GENERALIZED BLOCH SPHERE

We consider a nonlinear driven two-level model including a second-order nonlinearity as a (1:2) resonance (appearing in the coupling term) [25]:

$$i\dot{b}_1 = \frac{\Omega}{\sqrt{2}}\bar{b}_1 b_2, \tag{1a}$$

$$i\dot{b}_2 = (\Delta - \Lambda_a + 2\Lambda_s|b_2|^2)b_2 + \frac{\Omega}{2\sqrt{2}}b_1^2, \tag{1b}$$

with the amplitude probabilities b_1 and b_2 satisfying $|b_1|^2 + 2|b_2|^2 = 1$, i.e., with the nonlinearity associated to state 2. The time-dependent driving field couples the two states via its Rabi frequency $\Omega \equiv \Omega(t)$ (assumed positive for simplicity and without loss of generality) in a near-resonant way, and a detuning $\Delta \equiv \Delta(t)$. Additional third-order nonlinearities are considered as diagonal terms through the coefficients Λ_a and Λ_s (known as Kerr terms). In the language of Bose-Einstein condensation, this system (1) models the transfer from atomic to molecular condensates, where $|b_1|^2$ $(2|b_2|^2)$ is the probability of atomic (molecular) BEC. The term Λ_a can be trivially compensated by a static detuning, while the Λ_s term can be dynamically compensated by a time-dependent detuning, in a similar way as the one presented in Ref. [29] for the three-state problem.

Similarly to the linear counterpart, the dynamics of this nonlinear system can be parametrized by three angles $\theta \in [0, \pi]$, $\alpha \in [0, 2\pi[$, $\gamma \in [0, 2\pi[$ as [24,30]:

$$\begin{bmatrix} b_1(t) \\ b_2(t) \end{bmatrix} = \begin{bmatrix} \cos(\theta/2) \\ \frac{1}{\sqrt{2}}\sin(\theta/2)\, e^{-i(\alpha+\gamma)} \end{bmatrix} e^{-i\gamma}. \tag{2}$$

The problem can be reformulated with the (complex) Hamilton equations

$$\dot{b}_j = \frac{\partial h}{\partial \bar{b}_j}, \; j = 1, 2, \tag{3}$$

with the Hamiltonian [24,25]

$$h = \big(\Delta - \Lambda_a + \Lambda_s|b_2|^2\big)|b_2|^2 + \frac{\Omega}{2\sqrt{2}}\big(b_1^2\bar{b}_2 + \bar{b}_1^2 b_2\big). \tag{4}$$

Canonical transformations into the variables defining the phase space $(I = |b_2|^2, \alpha)$ lead to the coordinates, involving population inversion and the generalized coherence:

$$\Pi_z := |b_1|^2 - 2|b_2|^2 = 1 - 2p, \tag{5a}$$

$$\Pi_x := 2\big(b_1^2\bar{b}_2 + \bar{b}_1^2 b_2\big) = 2\sqrt{2}(1-p)\sqrt{p}\cos\alpha, \tag{5b}$$

$$\Pi_y := -2i\big(b_1^2\bar{b}_2 - \bar{b}_1^2 b_2\big) = 2\sqrt{2}(1-p)\sqrt{p}\sin\alpha, \tag{5c}$$

with twice state-2 population $p = 2I = 2|b_2|^2 = \sin^2(\theta/2)$. For convenience, one can alternatively consider the z coordinate as p instead of Π_z. The phase space can be reduced to a two-dimensional surface, defined as the generalized Bloch sphere, of equation

$$\Pi_x^2 + \Pi_y^2 = 8(1-p)^2 p, \; p \in [0, 1], \tag{6}$$

embedded in the three-dimensional space of coordinates Π_x, Π_y, p, as shown in Fig. 1. The south and north poles correspond, respectively, to $p = 0$ and $p = 1$.

The nonlinear Schrödinger equation leads to the following system of equations:

$$\dot{\theta} = \Omega\sin\alpha\cos(\theta/2), \quad \text{or} \quad \dot{p} = \Omega(1-p)\sqrt{p}\sin\alpha \tag{7a}$$

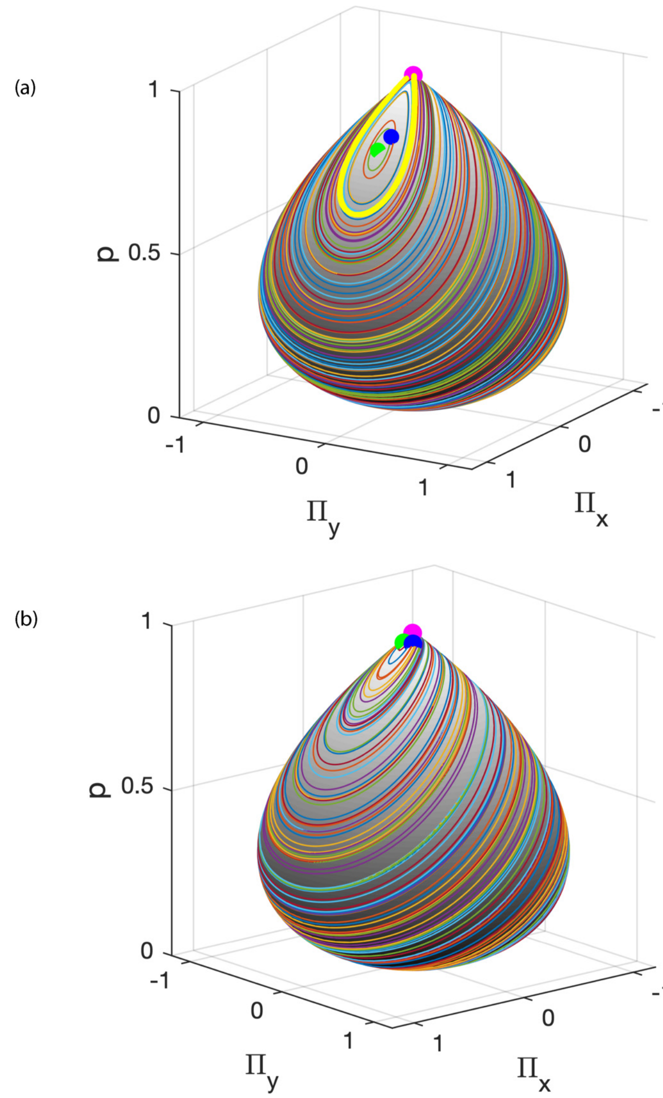

FIG. 1. Portraits of the system on the generalized Bloch sphere in the late part of the dynamics ($t = 1.2T$) for adiabatic tracking and robust control (with parameters of Fig. 4), including an additional static detuning (a) $T\Delta_0 = -0.6$ and (b) $T\Delta_0 = 0.6$, the separatrix (thick yellow line), elliptic fixed point (green dot), actual dynamics for adiabatic tracking (blue dot) and for robust control (magenta dot). At the chosen time, the values of the instantaneous detuning $\Delta(t)$ and of the Rabi frequency $\Omega(t)$ are almost identical in the two techniques, thus leading to the same portraits for each Δ_0.

$$\dot{\alpha} = \frac{\Omega}{2}\cos\alpha\frac{1-3\sin^2(\theta/2)}{\sin(\theta/2)} + \Delta - \Lambda_a + \Lambda_s\sin^2(\theta/2), \tag{7b}$$

$$\dot{\gamma} = \frac{\Omega}{2}\cos\alpha\sin(\theta/2), \tag{7c}$$

which can be rederived with $\dot{\alpha} = \partial h/\partial I$, $\dot{I} = \partial h/\partial \alpha$, and the Hamiltonian expressed with the phase space variables

$$h = (\Delta - \Lambda_a + \Lambda_s p/2)p/2 + \frac{\Omega}{2}(1-p)\sqrt{p}\cos\alpha. \tag{8}$$

From Eq. (7a) the population $p(t)$ can be written in terms of the angle $\alpha(t)$ as

$$p(t) = \tanh^2\left[\int_{t_i}^{t}\frac{\Omega(s)}{2}\sin\alpha(s)\,ds\right], \tag{9}$$

where we have assumed an initial state $b_1(t_i) = 1$ at the initial time t_i, i.e., $p(t_i) = 0$ (corresponding to the south pole of the generalized Bloch sphere in Fig. 1). We consider the target of a complete population transfer $p(t_f) = 1$ (corresponding to the north pole of the generalized Bloch sphere in Fig. 1) at the final time t_f. This shows that the transfer probability p can tend to one only in the limit of an infinite pulse area, in agreement with the time-optimal solution [28]. The Rabi model (for $\Delta = \Lambda_a$ and $\Lambda_s = 0$, i.e. $\alpha = \pi/2$) gives a high-fidelity transfer, robust with respect to the pulse area (unlike its linear counterpart), but strongly sensitive to a detuning $\Delta \neq 0$ (or equivalently to a third-order nonlinearity). It indeed induces oscillations in the integral of $p(t)$, which are more intense for a larger pulse area. The corresponding trajectory evolves on the separatrix associated to the target state $p = 1$, which is a hyperbolic fixed point.

III. NONROBUSTNESS OF ADIABATIC PASSAGE

We can limit our study for simplicity without third-order nonlinearities ($\Lambda_a = \Lambda_s = 0$), since this system already features an unstable target. The adiabatic trajectory is formed by the instantaneous stable (elliptic) fixed points among the fixed points defined by $\dot{I} = 0$, $\dot{\alpha} = 0$:

$$\Delta = -e^{i\alpha}\frac{\Omega}{2\sqrt{p}}(1-3p), \qquad \alpha = 0 \text{ or } \pi, \tag{10}$$

at each value of the adiabatic parameters Ω and Δ, and continuously connected to the initial condition $p = 0$. An adiabatic tracking trajectory is derived by imposing for instance convenient $p(t)$ and $\Omega(t)$, and using $\Delta(t)$ resulting from (10) [24,25].

The target $p = 1$ is a fixed point of the dynamics, which is hyperbolic for $|\Delta/\Omega| < 1$ and elliptic for $|\Delta/\Omega| > 1$. The number and the nature of the fixed points change as a function of Ω and Δ: (i) for $\Omega = 0$ and any Δ there are only two fixed points $p = 0$ and $p = 1$, which are both elliptic; (ii) for $\Omega \neq 0$: if $|\Delta/\Omega| < 1$ there are three fixed points: $p = 1$, which is hyperbolic, and two elliptic ones. If $|\Delta/\Omega| \geqslant 1$ there are two fixed points, both elliptic.

The separatrix associated to the hyperbolic fixed point is the curve of constant h passing by the hyperbolic fixed point $p = 1$ of the equation

$$(p_s - 1)(\Delta - \Omega\sqrt{p_s}\cos\alpha_s) = 0, \tag{11}$$

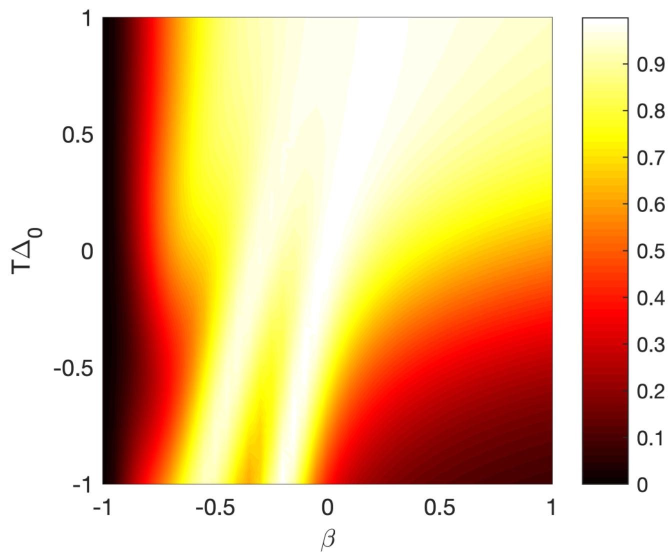

FIG. 2. Contour plot of the final population transfer $p(+\infty)$ for the adiabatic tracking $\Omega(t) = \Omega_0$ sech(t/T) and $p_{\rm track}(t) = \sin^2\{\arctan[\sinh(t/T)]/2 + \pi/4\}$ [24] with $T\Omega_0 = 10$ (and T the characteristic duration of the process) with respect to deviations of the detuning by a static quantity Δ_0 (in units of $1/T$) and of the field amplitude by $1+\beta$.

i.e.,

$$\sqrt{p_s}\cos\alpha_s = \Delta/\Omega = e^{i\alpha}(1-3p_0)/(2\sqrt{p_0}),\ \ \alpha = 0 \text{ or } \pi, \tag{12}$$

when $|\Delta/\Omega| < 1$ [see Fig. 1(a)]. When $|\Delta/\Omega|$ approaches 1 from below, the separatrix collapses to a single point and $p = 1$ becomes elliptic [see Fig. 1(b)].

The issue of robustness of a typical adiabatic tracking dynamics with respect to a static detuning Δ_0 and to the Rabi frequency amplitude is numerically analyzed in Fig. 2. This shows that the fidelity dramatically decreases for negative detuning Δ_0 and positive β, while it is relatively preserved on the other three quadrants. In what follows, we describe the dynamics in the phase space and provide a qualitative explanation of this global lack of robustness.

In order to reach the target $p = 1$ (north pole) by an adiabatic process, the trajectory must follow continuously the instantaneous elliptic fixed points that connect $p = 0$ (south pole) when $\Omega = 0$ (initially) to $p = 1$ when $\Omega/\Delta = 1$ (finally) without crossing a separatrix [22,24], as it is shown in Fig. 3(b). The initial state $p = 0$ corresponds to $\Delta/\Omega \to -\infty$ and the target $p = 1$ to $\Delta/\Omega \geqslant 1$. The intermediate state $p = 1/3$ corresponds to $\Delta/\Omega = 0$. Thus Δ necessarily has to go through 0. In the adiabatic tracking technique Δ is chosen such that $\Delta/\Omega \to 1$ from below at final time. If $\Delta/\Omega = 1$ at some finite time, the elliptic fixed point collides with the hyperbolic one, and the separatrix collapses to a single point. If there is an additional static detuning $\Delta_0 \neq 0$ there are two scenarios, depending on the sign of Δ_0. We assume without loss of generality that the initial $\Delta(t_i) < 0$ and thus at the approach of the target $\Delta > 0$. (i) If $\Delta_0 > 0$, then $(\Delta + \Delta_0)/\Omega$ goes through 1 at some finite time, then the elliptic and the hyperbolic points collide, the separatrix collapses, and $p = 1$ becomes elliptic [see Fig. 1(b)]. Since

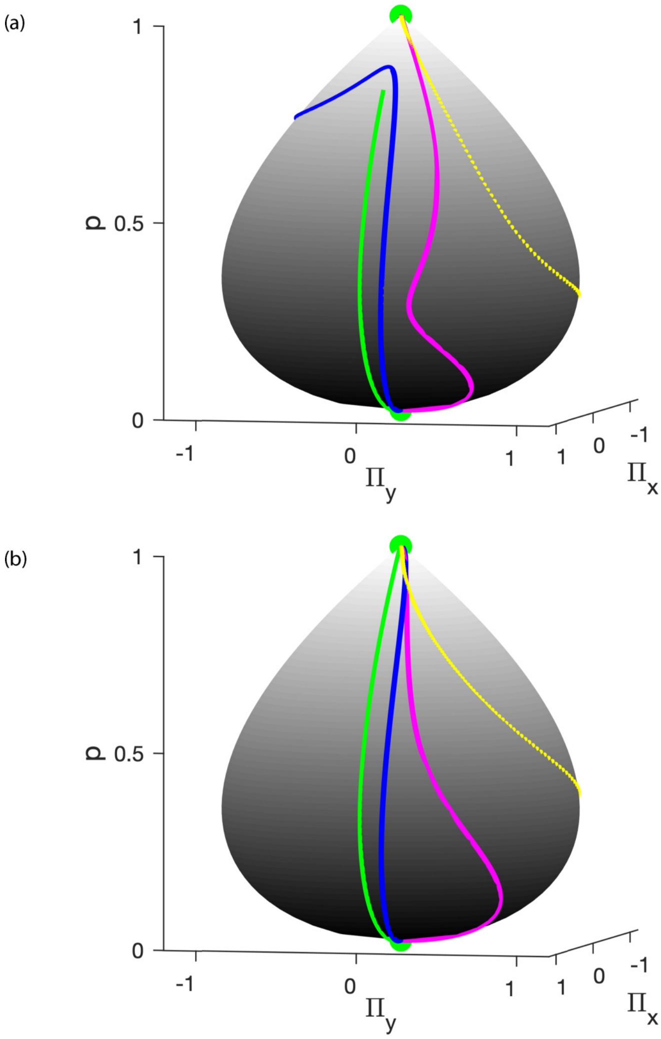

FIG. 3. Trajectories with the parameters of Fig. 1, followed by the dynamics from the south pole (initial condition) to north, with (a) a static detuning $T\Delta_0 = -0.6$ and (b) no static detuning $T\Delta_0 = 0$; trajectory of the instantaneous fixed points (green curves) associated to the adiabatic tracking dynamics, which connects the initial and target fixed points (green dots) in (b), but does not reach the target in (a); actual trajectory for adiabatic tracking (blue curves) adiabatically following the green fixed point trajectory (except at the end of the dynamics in (a), when the adiabatic connectivity fails); actual trajectory for robust control field (magenta curves) reaching the target closely to the separatrix at the approach of the target in both cases. The separatrix (yellow) curve is made by the points of the instantaneous separatrices, each of them having the same latitude p of the actual trajectory. The four trajectories almost merge at the target in (b).

$\Omega \neq 0$ this implies that the actual trajectory crosses the separatrix at some earlier time [see Fig. 3(b)] and the adiabatic approximation is broken. However, during the crossing the flow $\Pi_y > 0$ goes into the direction of the separatrix which points toward the target, according to (7a): $\dot{p} = \Omega\Pi_y/2\sqrt{2}$, despite a broken adiabatic approximation. This explains the relative robustness of the process for $\Delta_0 > 0$. (ii) If $\Delta_0 < 0$, since $[\Delta + \Delta_0]/\Omega < 1$, the elliptic fixed point stays at a finite distance from $p = 1$, i.e., the elliptic fixed point never reaches

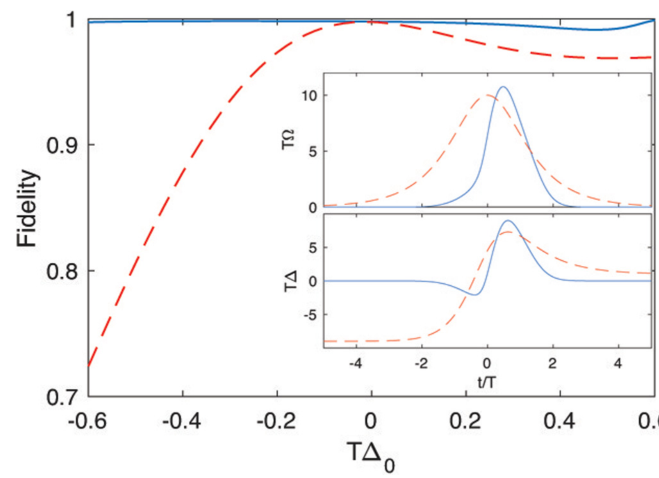

FIG. 4. Final transfer profile $p(+\infty)$ as a function of the static detuning Δ_0 (in units of $1/T$) showing (i) nonrobust adiabatic tracking (dashed red line) with the parameters of Fig. 2 for $\beta = 0$ and (ii) robust control (solid blue line) (16) with $C_1 = -0.5$, $C_{j>1} = 0$, and $\epsilon = 0.03$, of average transfer fidelity 0.997 in the zone of the figure. Inset: Corresponding pulse shapes of Rabi frequency (upper frame) and detuning (lower frame).

the target: the adiabatic connectivity is broken [see Figs. 1(a) and 3(a)]. We can state a similar explanation of nonrobustness of the Rabi frequency when it is multiplied by a coefficient larger than one. We can thus interpret this lack of robustness by the fact that the adiabatic connectivity is strongly sensitive to small perturbations of the model, which can be interpreted as a direct consequence of the instability of the target state.

IV. ROBUST CONTROL

We derive robust solutions on the basis of reverse engineering by adapting the technique developed for linear models in Ref. [8]. We assume a convenient time variation

$$\theta(t) = \frac{\pi}{2}(1-\epsilon)[1+\mathrm{erf}(t/T)] \tag{13}$$

(where $\epsilon = 0.03 > 0$ takes into account that the solution cannot reach the target state exactly), and we define an expansion of the phase γ as a function of θ, $\tilde{\gamma}(\theta) \equiv \gamma(t)$, with n unknown constants, C_j, $j = 1\ldots, n$:

$$\tilde{\gamma}(\theta) = \theta + C_1\sin(\theta) + C_2\sin(2\theta) + \cdots + C_n\sin(n\theta). \tag{14}$$

We determine α from (7c) and (7b) by eliminating Δ and replacing Ω using (7a), giving a differential equation for α as a function of θ, $\tilde{\alpha}(\theta) \equiv \alpha(t)$:

$$\dot{\tilde{\alpha}} = \frac{1}{\tan\tilde{\alpha}\sin\theta} - 3\dot{\tilde{\gamma}}, \tag{15}$$

where $\tilde{\alpha}(0) = \pm\pi/2$ for $\theta = 0$. The field shaping is then determined from (7a) and (7c), respectively:

$$\Omega(t) = \frac{\dot{\theta}}{\sin\alpha\cos(\theta/2)}, \tag{16a}$$

$$\Delta(t) = \frac{3}{2}\cot\alpha\tan(\theta/2) - 3\dot{\gamma} + \Lambda_a - \Lambda_s\sin^2(\theta/2). \tag{16b}$$

We have to determine numerically the coefficients C_j's leading to a desired robust transfer.

Figure 4 shows the remarkable robustness achieved with respect to the static detuning Δ_0 for $C_1 = 0.5$ and $C_{j>1} = 0$ and the corresponding pulse and detuning shapes. It surpasses the robustness of adiabatic tracking with twice the lower Rabi frequency area (5π and 10π, respectively). The robustness of this derived trajectory is analyzed in the phase space (see Fig. 3): The initial trajectory breaks the adiabaticity by starting orthogonally to the fixed point curve ($\Delta = 0$). When Ω reaches a sufficiently large value, the actual dynamics becomes adiabatic along a trajectory that is not close to the elliptic fixed points, until approaching a region near the separatrix. The stable manifold of the separatrix drives then all the trajectories in its vicinity towards the target, thus in a robust way.

V. CONCLUSION

We have shown that adiabatic passage in nonlinear quantum systems is not robust when the target point is unstable due to the sensitivity to small perturbations of the adiabatic connectivity. We have developed alternative robust trajectories that circumvent the instability. The main difference is that adiabatic tracking tries to follow closely the instantaneous fixed points, while the robust control field method operates quite far away from the fixed points near the separatrix and the stable manifold, breaking adiabaticity at the beginning of the process. Inverse engineering is usually applied in the context of (linear) quantum control to make a process exact, fast, and/or robust. In this paper we have shown that inverse engineering also allows remarkably circumvention of a nonlinear instability.

We remark that usual nonlinear STIRAP-type processes [29] are not affected by this lack of robustness as the target state, linked with the linear Stokes coupling, is stable. This is also the case for two-level systems featuring only third-order nonlinearity [28].

The present control has been designed to be robust with respect to detuning (or equivalently to third-order nonlinearities). Robustness with respect to pulse amplitude or to both amplitude and detuning requires other parametrizations. We have determined that the coefficients $C_1 = -2.05$, $C_2 = -1$, $C_3 = 0.35$, $C_{j>3} = 0$ lead to an averaged fidelity of 0.964 in the range $-1 \leqslant T\Delta_0 \leqslant 1$, $-0.1 \leqslant \beta \leqslant 0.1$ (to be compared to the one of adiabatic passage 0.86). We notice that the chosen form of parametrization does not improve much the robustness with respect to the pulse amplitude.

These results can be immediately applicable to superchemistry [15,31,32] and other scenarios, including frequency conversion beyond the undepleted pump approximation [21], nonlinear coupled waveguides [33], and nonlinear Landau-Zener problems for a Bose-Einstein condensate in an accelerating optical lattice [34]. Last but not least, the success of inverse engineering and shortcuts to adiabaticity applied for nonlinear systems opens the possibility of extending shared concepts such as dynamical or adiabatic invariants and fast-forward scaling [12,13].

ACKNOWLEDGMENTS

This work was partially supported by the NSFC (11474193), SMSTC (18010500400, 18ZR1415500, and 2019SHZDZX01-ZX04), and the Program for Eastern Scholar. X.C. also acknowledges the Ramón y Cajal program of the Spanish MCIU (RYC-2017-22482). S.G. and H.-R.J. acknowledge additional support by the French "Investissements d'Avenir" programs, project ISITE-BFC/I-QUINS (contract ANR-15-IDEX-03), QUACO-PRC (Grant No. ANR-17-CE40-0007-01), EUR-EIPHI Graduate School (17-EURE-0002), and from the European Union's Horizon 2020 research and innovation program under the Marie Sklodowska-Curie Grant Agreement No. 765075 (LIMQUET).

[1] J. P. Dowling and G. Milburn, Philos. Trans. R. Soc. London A **361**, 1655 (2003).
[2] C. Brif, R. Chakrabarti, and H. Rabitz, New J. Phys. **12**, 075008 (2010).
[3] N. V. Vitanov, A. A. Rangelov, B. W. Shore, and K. Bergmann, Rev. Mod. Phys. **89**, 015006 (2017).
[4] M. H. Levitt, *Spin Dynamics: Basics of Nuclear Magnetic Resonance* (John Wiley & Sons, New York, 2008).
[5] G. T. Genov, D. Schraft, T. Halfmann, and N. V. Vitanov, Phys. Rev. Lett. **113**, 043001 (2014).
[6] N. Khaneja, T. Reiss, C. Kehlet, T. Schulte-Herbrggen, and S. J. Glaser, J. Magn. Reson. **172**, 296 (2005).
[7] T. Nöbauer, A. Angerer, B. Bartels, M. Trupke, S. Rotter, J. Schmiedmayer, F. Mintert, and J. Majer, Phys. Rev. Lett. **115**, 190801 (2015).
[8] D. Daems, A. Ruschhaupt, D. Sugny, and S. Guérin, Phys. Rev. Lett. **111**, 050404 (2013).
[9] L. Van-Damme, D. Schraft, G. T. Genov, D. Sugny, T. Halfmann, and S. Guérin, Phys. Rev. A **96**, 022309 (2017).
[10] X. Chen, I. Lizuain, A. Ruschhaupt, D. Guéry-Odelin, and J. G. Muga, Phys. Rev. Lett. **105**, 123003 (2010).
[11] A. Ruschhaupt, X. Chen, D. Alonso, and J. G. Muga, New J. Phys. **14**, 093040 (2012).
[12] E. Torrontegui, S. Ibánez, S. Martínez-Garaot, M. Modugno, A. del Campo, D. Guéry-Odelin, A. Ruschhaupt, X. Chen, and J. G. Muga, Adv. At. Mol. Opt. Phys. **62**, 117 (2013).
[13] D. Guéry-Odelin, A. Ruschhaupt, A. Kiely, E. Torrontegui, S. Martínez-Garaot, and J. G. Muga, Rev. Mod. Phys. **91**, 045001 (2019).
[14] L. Pitaevskii and S. Stringari, *Bose-Einstein Condensation* (Clarendon Press, Oxford, 2003).
[15] M. Mackie, R. Kowalski, and J. Javanainen, Phys. Rev. Lett. **84**, 3803 (2000).
[16] L. D. Carr, D. DeMille, R. V. Krems, and J. Ye, New J. Phys. **11**, 055049 (2009).
[17] R. W. Boyd, *Nonlinear Optics* (Academic Press, Orlando, FL, 2008).
[18] G. P. Agrawal, *Nonlinear Fiber Optics* (Academic Press, New York, 2007).

[19] S. Longhi, Opt. Lett. **32**, 1791 (2007).
[20] Y. Lahini, F. Pozzi, M. Sorel, R. Morandotti, D. N. Christodoulides, and Y. Silberberg, Phys. Rev. Lett. **101**, 193901 (2008).
[21] H. Suchowski, G. Porat, and A. Arie, Laser Photonics Rev. **8**, 333 (2014).
[22] A. P. Itin and S. Watanabe, Phys. Rev. Lett. **99**, 223903 (2007).
[23] A. Dey, D. Cohen, and A. Vardi, Phys. Rev. Lett. **121**, 250405 (2018).
[24] S. Guérin, M. Gevorgyan, C. Leroy, H. R. Jauslin, and A. Ishkhanyan, Phys. Rev. A **88**, 063622 (2013).
[25] M. Gevorgyan, S. Guérin, C. Leroy, A. Ishkhanyan, and H. R. Jauslin, Eur. Phys. J. D **70**, 253 (2016).
[26] U. Boscain, G. Charlot, J.-P. Gauthier, S. Guérin, and H. R. Jauslin, J. Math. Phys. **43**, 2107 (2002).
[27] B. Bonnard, D. Sugny, *Optimal Control with Applications in Space and Quantum Dynamics*, AIMS on Applied Mathematics (American Institute of Mathematical Sciences, Springfield, MA, 2012), Vol. 5.
[28] X. Chen, Y. Ban, and G. C. Hegerfeldt, Phys. Rev. A **94**, 023624 (2016).
[29] V. Dorier, M. Gevorgyan, A. Ishkhanyan, C. Leroy, H. R. Jauslin, and S. Guérin, Phys. Rev. Lett. **119**, 243902 (2017).
[30] K. Efstathiou, *Metamorphoses of Hamiltonian Systems with Symmetries*, Lecture Notes in Mathematics (Springer-Verlag, Berlin, 2005), Vol. 1864.
[31] J. J. Hope and M. K. Olsen, Phys. Rev. Lett. **86**, 3220 (2001).
[32] M. G. Moore and A. Vardi, Phys. Rev. Lett. **88**, 160402 (2002).
[33] R. Khomeriki, Phys. Rev. A **82**, 013839 (2010).
[34] B. Wu and Q. Niu, Phys. Rev. A **61**, 023402 (2000).